Track 1: Machine Design

A Constant Force Mechanism based Vibration Isolator for Low-Frequency Excitations

Srajan Dalela[1#], Akash Prasad Sahoo[1], Pyla Prasad[1], P. S. Balaji[1]

[1]Department of Mechanical Engineering, National Institute of Technology, Rourkela 769008, India

[#]Corresponding author: 518me1016@nitrkl.ac.in

srajandalela@gmail.com

Abstract

In this work a constant force mechanism (CFM) is proposed to regulate the contact force of a robot end effector. A robotic arm is designed that possess constant force for certain range of displacement, and the vibration can be isolated in the specified displacement range. A numerical study is proposed in this work for studying the static and dynamic behaviour. Firstly, the static characteristics is performed to obtain the operational displacement range where the reaction force is maintained nearly constant. The static analysis results are then used as the input for the studying the dynamic characteristics. The nonlinear dynamic performance is evaluated using the harmonic and transient modules. A parametric study is also performed to evaluate the effects of varying damping ratio. The results suggest a constant reaction force for certain displacement range, and the effective isolation is also obtained for the low-frequency ranges.

Keywords: Constant force mechanism (CFM), metastructure, HSLDS, robotic arm

1. Introduction

Vibration is pivotal to many real-world engineering applications due to its deleterious effects on system performance and affects the system's ability to accomplish the desired operation. So with a view to controlling the impedance of the vibration, various vibration mitigation methods have been adopted and one of them is passive vibration isolation that can help in achieving the isolation by utilising tuned vibration absorbers, tuned mass dampers, linear and nonlinear vibration isolation system that prevent external excitation from being moved to the system by alienating the object of interest from the source of excitation.

For wide range of low excitation frequencies, non-linear vibration isolators are more effective than linear isolator as it has a characteristic of high static and low dynamic stiffness. Here, high static stiffness refers to high values of static load-carrying capacity undergoing low displacement, whereas the low-dynamic stiffness refers to increased excitation isolation region at low excitation frequencies. Ibrahim's review work [1] examines different nonlinear isolators and shows that progress in nonlinear isolators is a very active area.

The nonlinear isolator has a distinguishing feature of nearly zero dynamic stiffness, also termed as the Quasi-zero stiffness characteristic, which specifies a nearly constant reactive force by the isolator across a specified displacement range. By counterbalancing positive stiffness, negative stiffness elements in the nonlinear isolator have a significant role in the formation of QZS characteristic [2-6]. The negative stiffness feature can be implemented using a variety of structures, including oblique or inclined springs [7, 8], buckled beams [9], bi-stability based structures [10-12], magnetic springs [13-15], and bio-mimetic structures [16, 17]. The constant force mechanism (CFM) is a nonlinear isolation mechanism with quasi-zero stiffness characteristic that is designed and assessed for vibration isolation in the paper. The variation of the reactive force by the mechanism is confined in the operating range of displacement, hence it is termed constant force mechanism (CFM). The internal periodic configuration of CFM determines its unique qualities rather than the intrinsic properties of solid materials. CFM has several benefits, such as its ability to return to original shape and absorb mechanical energy consistently due to the external excitation.

Constant-force and constant-torque springs consisting of one or more coiled strips of spring steel are good examples. These are frequently used in retrieving wires, counterbalancing the weight, and adjusting the lengths. The simplest possible CFM relies on elastic structures buckling and as an illustration Sönmez [18] developed a buckled beam and arc-based compliant dwell mechanism. Aside from buckling, the incorporation of positive and negative stiffness elements benefits the majority of other CFMs. This method can be used to transform standard linkages to CFMs by incorporating torsional and/or linear springs [19, 20]. Boyle *et al.* [21] also proposed a leaf spring-based constant-force compression mechanism. A constant-force double-slider method was implemented by Nahar and Sugar [22]. By adjusting the spring length, the mechanism's force magnitude can be adjusted. CFMs, for its enhanced ability of non-linear isolation, preferred to be made of one type of material for miniaturisation. Pedersen *et al.* [23] developed a monolithic compliant mechanism with a constant force output.

The focus of this article is to construct a CFM with near-zero dynamic stiffness and investigate its properties in vibration reduction scenarios. Static characteristics under uniaxial vertical displacement have been investigated and dynamic behaviour of the CFM has been studied through numerous simulation analyses. Acceleration transmissibility index was used to assess the vibration isolation capability of the designed CFM. The results suggest that the given CFM has outstanding excitation isolation capabilities and has a lot of potential to be used in small-scale equipment for vibration isolation.

2. Structural Model

In Figure 1a, each beam of the sub-CFM, enclosed in *(10*8*6) mm³* design box, has a rectangular cross-section with an in-plane thickness of *w* and an out-of-plane thickness of *t*. Each beam's flexural rigidity is indicated by *EI*, where *E* indicates the elastic property and $I = tw^3/12$ gives the area moment of inertia of the section of each beam. The beam model is shown in Fig. A shape (intrinsic) function $\eta(u)$ is used to characterize the un-deformed beam, where $u \in [0\ 1]$ is a non-dimensional arc length along the length of un-deformed curved beam and η quantifies the angle of rotation (in radians) along *u*.

On the neutral axis of each beam (shown in Figure 1c) , any arbitrary point of *[x (u) y (u)]* is expressed as [24]-

$$x(\hat{u}) = x(0) + L\int_0^{\hat{u}} \cos\eta du \quad ; \quad y(\hat{u}) = y(0) + L\int_0^{\hat{u}} \sin\eta du \tag{1}$$

Where L represents the length of beam. The un-deformed forms of the three beams in a sub-CFM, as described by the shape function η, are parameterized using polynomials [25] as follows for convenience.

Table 1. Represents the equation used to define the model

Position (cm)	Shape function (rad)	Length(cm)
n_1= [1,0.2]	η_1=1.6401+0.9920u-1.5706u²	L_1=0.360
n_2= [0.99,0.55]	η_2=3.2380-0.8791u+0.7358u²	L_2=0.849
n_3= [0.15,0.64]	η_3=2.4429-1.1268u+0.2199u²	L_3=0.407
n_4= [0,1]		

The node points linking the three beams are n_1, n_2, n_3, and n_4 and during the generation of each beam, they are considered as the starting point. And *w=0.4 mm* and *t=6 mm* are the in-plane and out-of-plane thicknesses, respectively. The position of the node points and shape functions are as per [25].

The model is prepared as illustrated in the Figure 1a, it is designed in order to maintain the structural stability and to keep the resonance frequency low which leads to the better vibration isolation against low frequency external excitation.

3. Static Analysis

The current section discusses the results of static and dynamic analysis of the Metastructure. Force-Displacement graphs, and frequency response at different values of damping ratio are plotted and the

transmissibility is also studied at different values of damping ratio by giving base excitation. One of the important factors in studying of vibration isolation is transmissibility which was calculated from both harmonic and transient analysis.

Finite Element Analysis (FEA) based simulation is conducted in ANSYS 19R3 to study the mechanical properties of the Metastructure and the geometry is modeled using SOLIDWORKS 2020 software. Static structural analysis is performed in ANSYS with meshing using tetrahedron elements for compression tests (167,826 nodes and 77,558 elements). A nonlinear adaptive region is included with re-meshing criterion to obtain the better accuracy and refined mesh, as the large deformation is activated for the applied displacement. Boundary conditions are applied in such a way that the performed analysis will imitate the real time experiment. Bottom surface of the metastructure is fixed in all the six degrees of freedom (three translational and three rotational) and only compression in vertical direction is given for the top plate with a prescribed displacement whereas all the remaining five degrees of freedom are restricted. As the walls are made of harder material than that of nonlinear deforming elements in metastructure, stiffer walls are assumed to be rigid and hence constrained in all directions.

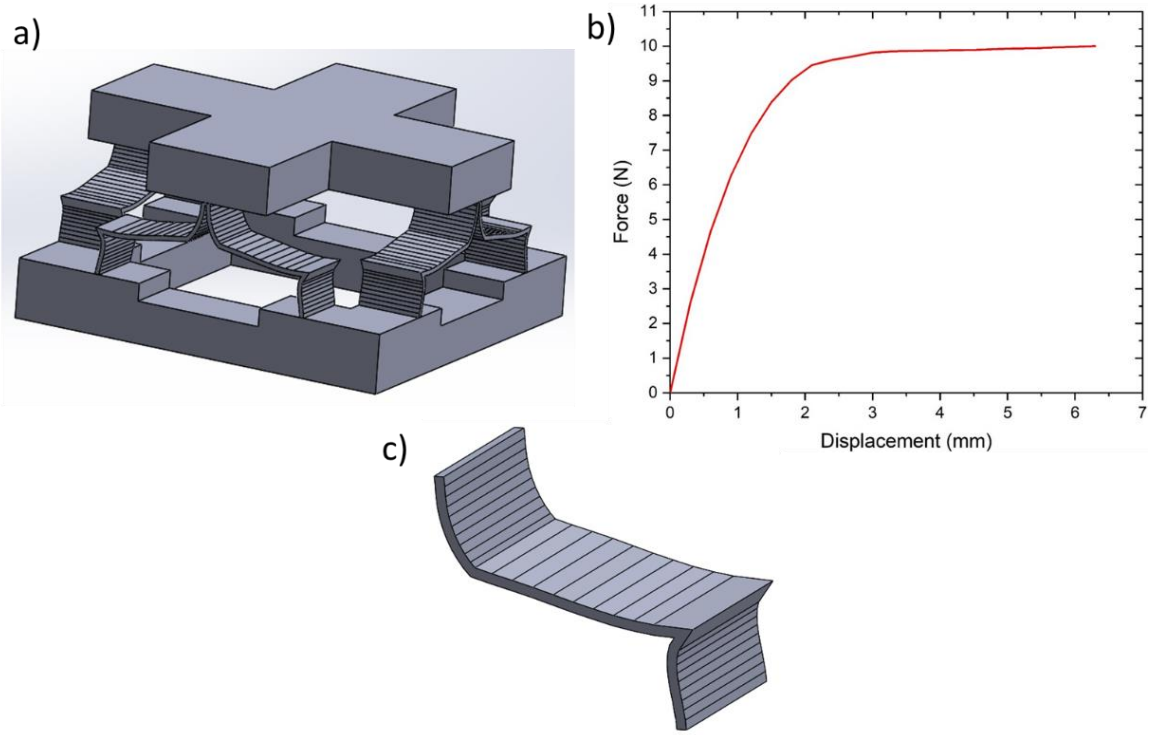

Figure 1. (a) Represents the 3D model, (b) Represents the force-displacement curve of the model, (c) Represents the beam used to model the unit cell.

Static Analysis of Metastructure is done using Ansys Workbench and the following force displacement graph is obtained as shown in Figure 1b. From the curve, it can be observed that the constant force of magnitude nearly 10N is obtained as soon as the system crosses a displacement of 3mm which is when the system enters quasi zero stiffness region. This region is our primary importance for vibration isolation applications because of low dynamic stiffness, whereas the region before quasi zero stiffness describes the static load carrying capacity of the system that justifies the mechanism High Static Low Dynamic Stiffness characteristics.

4. Dynamic Analysis

In static analysis, quasi zero stiffness region is obtained and the observed constant force is of 10N which is equivalent to 1.02 kg weight placing on the top of the Metastructure. Hence modal analysis is performed using the same mass placed on the top of Metastructure and different mode shapes with their frequencies are recorded as shown in Table 2.

Table 2: Frequencies recorded at different mode shapes.

Mode	Frequency (HZ)
1	8.3546
2	10.168
3	10.173
4	53.934
5	53.98
6	70.612

The current study is concerned about the vertical vibration of the model which is observed in mode shape 1 having the natural frequency of 8.35Hz. Using this natural frequency, Transient Analysis is performed by giving base excitation of $a = a_0 Sin(\omega t)$ mm/s^2, where a_0 corresponds to the excitation amplitude (800mm/s^2) and ω corresponds to the excitation frequency. Here the transient study is performed for varying excitation frequency (ω) and the responses are plotted in terms of Acceleration vs Time graphs. Figure 2, Figure 3 and Figure 4 corresponds to acceleration-time graph for different values of excitation frequencies with varying damping ratios.

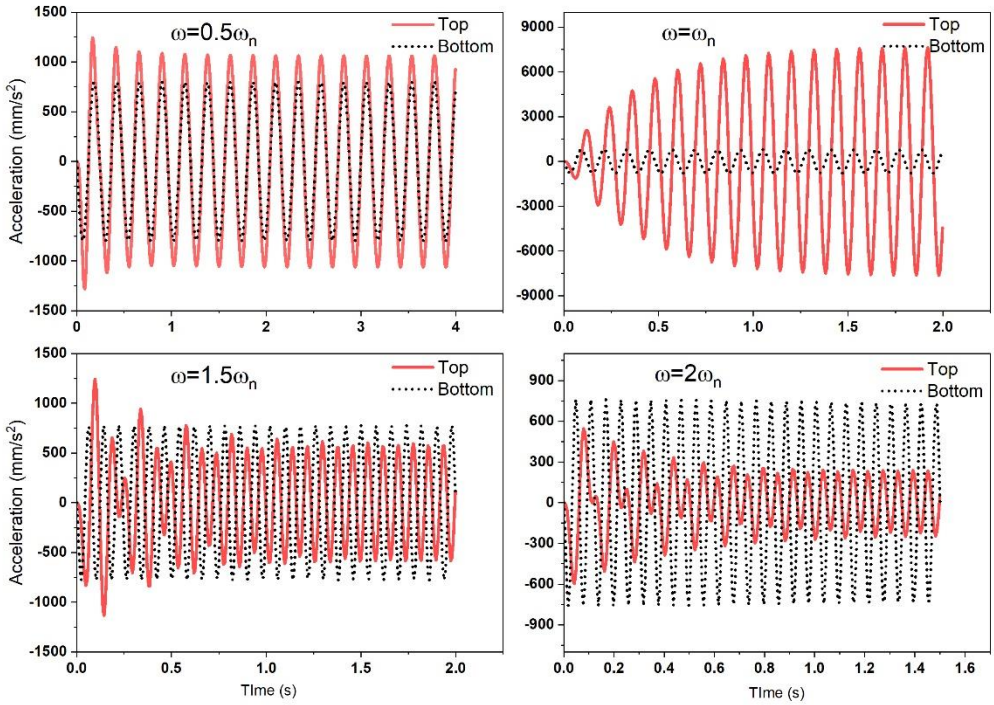

Figure 2: Acceleration vs Time plots at different base excitation frequency for damping ratio of 0.05.

It can be observed from the obtained curve that for lower values of excitation frequency ($\omega = 0.50\omega n$) reduction in output acceleration is not very significant, whereas for $\omega = 1.5\omega n$ significant reduction in output acceleration can be seen. Hence higher values of damping ratio can be preferred for vibration isolation applications. Transmissibility in case of transient analysis can be calculated by ratio of root mean square values of output amplitude to root mean square value of base excitation amplitude for the present study.

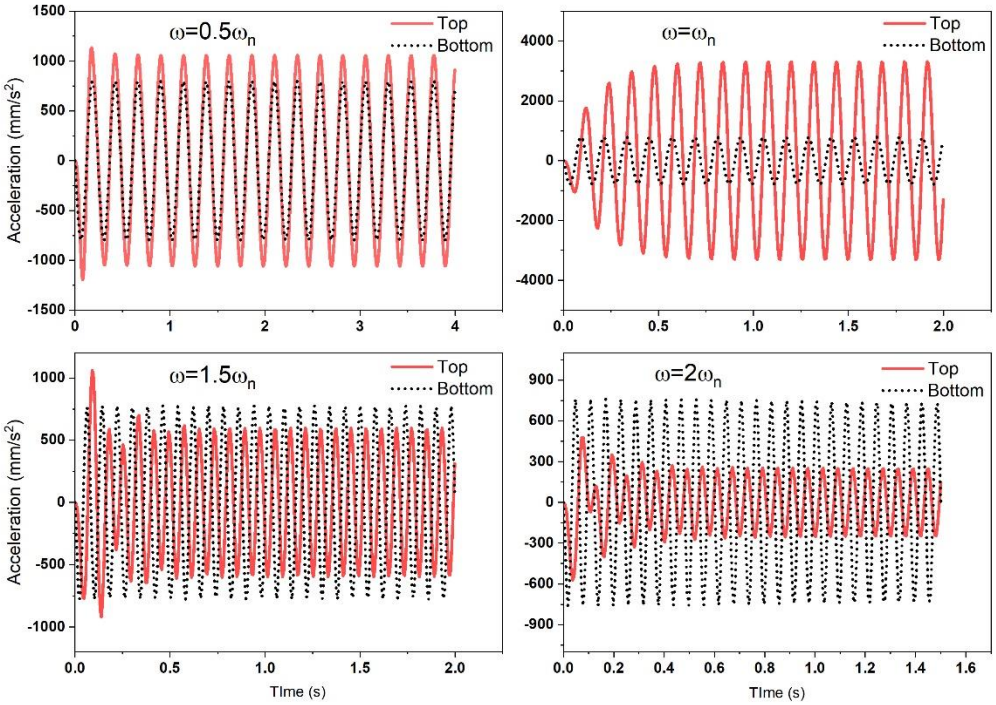

Figure 3: Acceleration vs Time plots at different base excitation frequency for damping ratio of 0.10.

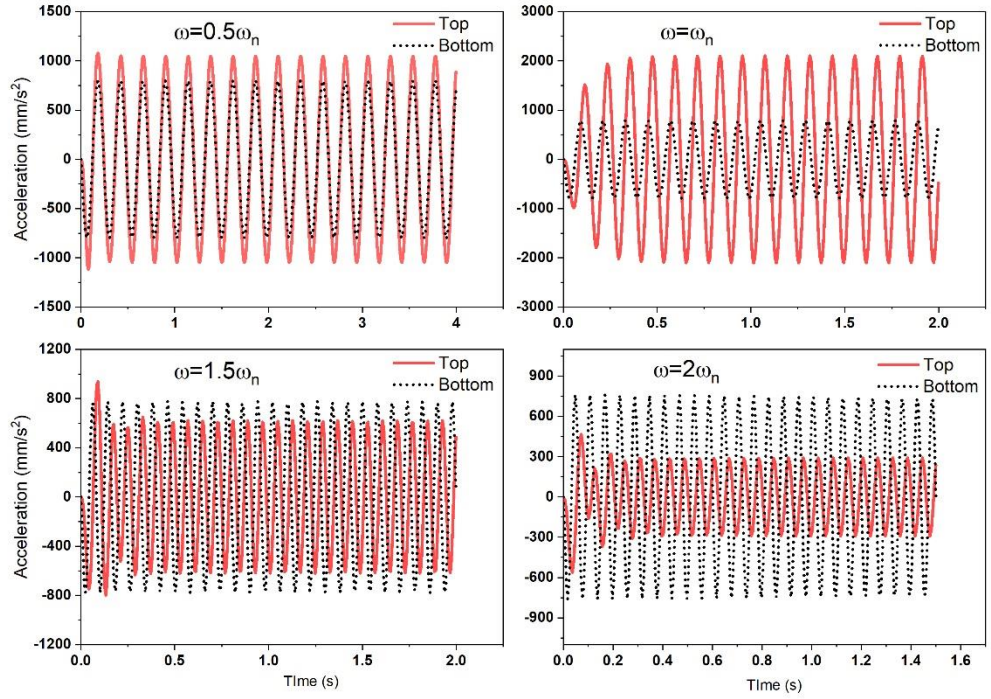

Figure 4: Acceleration vs Time plots at different base excitation frequency for damping ratio of 0.20.

Transmissibility in case of harmonic analysis for this study is = $\frac{Output\ Amplitude}{Input\ Amplitude}$ (2)

Transmissibility in case of transient analysis= $\sqrt{\frac{\sum a_0^2}{\sum a_i^2}}$ (3)

Where, a_o is the output amplitude and a_i is the input amplitude. Transmissibility values are calculated from the obtained acceleration values corresponding to the excitation frequencies.

Harmonic analysis is also performed in the linearised manner to study the behaviour of proposed model by giving base excitation with acceleration of $a = a_0 Sin(\omega t)$ mm/s^2, where a_0 corresponds to the excitation amplitude (800mm/s^2) and ω corresponds to the excitation frequency. Transmissibility(dB) vs Frequency graph is plotted at different damping ratios as shown in the Figure 5a.Figure 5: Transmissibility vs frequency obtained from harmonic analysis at different damping ratio It can be seen that transmissibility falls below zero once the excited frequency crosses 11.81Hz i.e.($\sqrt{2}\omega_n$). It can also be seen from Figure 5 that increasing damping ratio decreases the transmissibility peak at resonance frequency, but at higher frequency range the lower damping provides better isolation. Thus, it is advisable to use the damping ratio as per the required frequency range for vibration isolation applications.

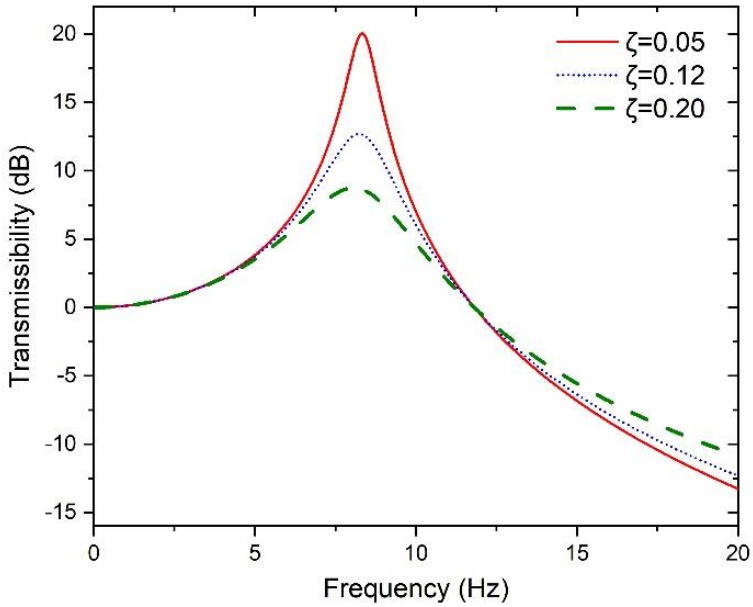

Figure 5: Transmissibility vs frequency obtained from harmonic analysis at different damping ratio.

Further the transmissibility calculated from the transient analysis based on the Equation 3, is plotted in FIGURE 6 and compared with that of harmonic results for different values of damping ratio. It can be observed that the curves of harmonic and transient analysis come in good agreement with each other.

5. Conclusion

- A 3D model is designed exhibiting constant force mechanism. Static analysis is performed and force vs displacement curve is plotted from structural analysis using Ansys Workbench in order to find the constant force region.
- Modal Analysis is performed to obtain the natural frequencies of the 3D model by using the force observed at constant force region as weight placed on top of the Metastructure.
- Harmonic analysis is conducted by giving base excitation and frequency response was plotted and compared with results from that of transient analysis. From transient and harmonic analysis, a significant reduction in the resonance peak is observed in case of higher value of damping ratio.
- Transmissibility curves plotted from harmonic and transient analysis are observed to be in good agreement with each other.

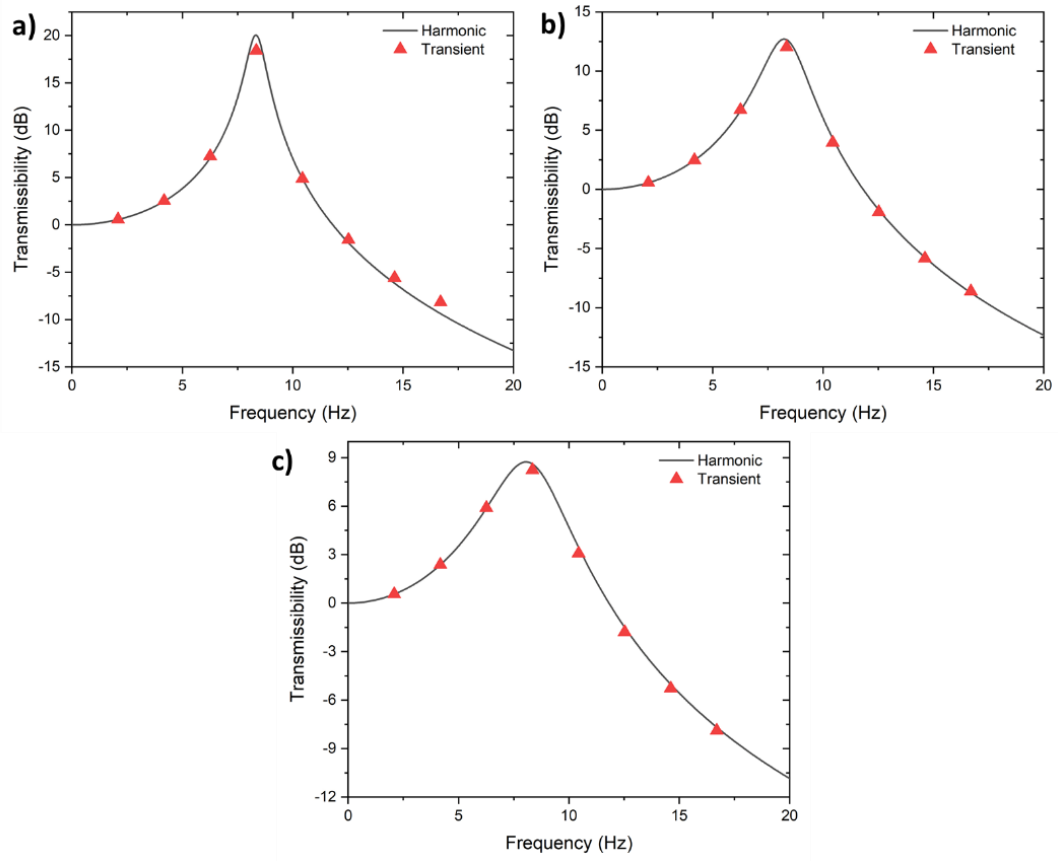

Figure 6. Transmissibility vs frequency curve showing comparison between harmonic and transient analysis results for different damping ratios- (a) 0.05, (b) 0.12, (c) 0.20.

Acknowledgement

This work is supported by the Science and Engineering Research Board (SERB), Department of Science and Technology (DST), India (Grant number-CRG/2021/002660), which is gratefully acknowledged.

References

1. Ibrahim, R., *Recent advances in nonlinear passive vibration isolators.* Journal of sound and vibration, 2008. **314**(3-5): p. 371-452.

2. Carrella, A., M. Brennan, and T. Waters, *Static analysis of a passive vibration isolator with quasi-zero-stiffness characteristic.* Journal of sound and vibration, 2007. **301**(3-5): p. 678-689.

3. Carrella, A., et al., *On the force transmissibility of a vibration isolator with quasi-zero-stiffness.* Journal of Sound and Vibration, 2009. **322**(4-5): p. 707-717.

4. Fulcher, B.A., Evaluation of systems containing negative stiffness elements for vibration and shock isolation. 2012.

5. Dalela, S., P. Balaji, and D. Jena, *A review on application of mechanical metamaterials for vibration control.* Mechanics of advanced materials and structures, 2021: p. 1-26.

6. Balaji, P. and K. Karthik SelvaKumar, *Applications of nonlinearity in passive vibration control: a review.* Journal of Vibration Engineering & Technologies, 2021. **9**(2): p. 183-213.

7. Lan, C.-C., S.-A. Yang, and Y.-S. Wu, *Design and experiment of a compact quasi-zero-stiffness isolator capable of a wide range of loads.* Journal of Sound and Vibration, 2014. **333**(20): p. 4843-4858.

8. Hao, Z. and Q. Cao, The isolation characteristics of an archetypal dynamical model with stable-quasi-zero-stiffness. Journal of sound and vibration, 2015. **340**: p. 61-79.

9. Huang, X., et al., Vibration isolation characteristics of a nonlinear isolator using Euler buckled beam as negative stiffness corrector: a theoretical and experimental study. Journal of Sound and Vibration, 2014. **333**(4): p. 1132-1148.

10. Vo, N. and T. Le, *Adaptive pneumatic vibration isolation platform.* Mechanical Systems and Signal Processing, 2019. **133**: p. 106258.

11. Ye, K., J. Ji, and T. Brown, *Design of a quasi-zero stiffness isolation system for supporting different loads.* Journal of sound and vibration, 2020. **471**: p. 115198.

12. Dalela, S., P. Balaji, and D. Jena, Design of a metastructure for vibration isolation with quasi-zero-stiffness characteristics using bistable curved beam. Nonlinear Dynamics, 2022: p. 1-41.

13. Yan, B., et al., *A bistable vibration isolator with nonlinear electromagnetic shunt damping*. Mechanical Systems and Signal Processing, 2020. **136**: p. 106504.

14. Zhu, T., et al., Vibration isolation using six degree-of-freedom quasi-zero stiffness magnetic levitation. Journal of Sound and Vibration, 2015. **358**: p. 48-73.

15. Robertson, W.S., et al., Theoretical design parameters for a quasi-zero stiffness magnetic spring for vibration isolation. Journal of Sound and Vibration, 2009. **326**(1-2): p. 88-103.

16. Jiang, G., X. Jing, and Y. Guo, *A novel bio-inspired multi-joint anti-vibration structure and its nonlinear HSLDS properties.* Mechanical Systems and Signal Processing, 2020. **138**: p. 106552.

17. Bian, J. and X. Jing, Superior nonlinear passive damping characteristics of the bio-inspired limb-like or X-shaped structure. Mechanical Systems and Signal Processing, 2019. **125**: p. 21-51.

18. Sönmez, Ü., Introduction to compliant long dwell mechanism designs using buckling beams and arcs. 2007.

19. Nathan, R., A constant force generation mechanism. 1985.

20. Weight, B.L., Development and design of constant-force mechanisms. 2002.

21. Boyle, C., et al., *Dynamic modeling of compliant constant-force compression mechanisms.* Mechanism and machine theory, 2003. **38**(12): p. 1469-1487.

22. Nahar, D.R. and T. Sugar. Compliant constant-force mechanism with a variable output for micro/macro applications. in 2003 IEEE International Conference on Robotics and Automation (Cat. No. 03CH37422). 2003. IEEE.

23. Pedersen, C., N. Fleck, and G. Ananthasuresh, Design of a compliant mechanism to modify an actuator characteristic to deliver a constant output force. 2006.

24. Lan, C.-C. and K.-M. Lee, Generalized shooting method for analyzing compliant mechanisms with curved members. 2006.

25. Lan, C.-C., J.-H. Wang, and Y.-H. Chen. A compliant constant-force mechanism for adaptive robot end-effector operations. in 2010 IEEE International Conference on Robotics and Automation. 2010. IEEE.